



**Mesoporous Silica-Supported Rhodium Complexes Alongside
Organic Functional Groups for Catalysing 1,4-Addition
Reaction of Arylboronic Acid in Water**

Journal:	<i>Green Chemistry</i>
Manuscript ID	GC-ART-12-2021-004577.R2
Article Type:	Paper
Date Submitted by the Author:	08-Mar-2022
Complete List of Authors:	Kong, Yuanyuan; Tokyo Institute of Technology, ; Yokohama National University, Department of Chemistry and Life Science Ding, Siming; Tokyo Institute of Technology, ; Yokohama National University, Department of Chemistry and Life Science Endo, Koichiro; Hokkaido University, Catalysis Research Center Nakajima, Kiyotaka; Hokkaido University, Catalysis Research Center; Japan Science and Technology Agency, PRESTO Manaka, Yuichi; National Institute of Advanced Industrial Science and Technology, Renewable Energy Research Center; Tokyo Institute of Technology, School of Materials and Chemical Technology Chun, Wang-Jae; International Christian University, Graduate School of Arts and Sciences Tomita, Ikuyoshi; Tokyo Tech, Motokura, Ken; Yokohama National University, Department of Chemistry and Life Science; Tokyo Institute of Technology,

ARTICLE

Mesoporous Silica-Supported Rhodium Complexes Alongside Organic Functional Groups for Catalysing 1,4-Addition Reaction of Arylboronic Acid in Water

Received 00th January 20xx,
Accepted 00th January 20xx

DOI: 10.1039/x0xx00000x

Yuanyuan Kong,^{a,b} Siming Ding,^{a,b} Koichiro Endo,^c Kiyotaka Nakajima,^c Yuichi Manaka,^{a,d} Wang-Jae Chun,^e Ikuyoshi Tomita,^a and Ken Motokura^{*a,b}

The 1,4-addition reaction of arylboronic acid catalysed using a Rh complex is critical in the synthesis of β -arylcabonyl compounds. However, most organic syntheses are performed in toxic organic solvents that pollute the environment. Conversely, water is cheap, non-toxic, abundant, and green. Therefore, improving the yield of the abovementioned 1,4-addition reaction in water is highly desirable. Here, Rh complexes and organic functional groups were co-immobilized on the internal surface of mesoporous silica with different mesopore diameters. The properties of the mesoporous silica-supported Rh catalysts were characterised using Fourier transform infrared spectroscopy, Rh *K*-edge X-ray absorption fine structure analysis, inductively coupled plasma atomic emission spectroscopy, CHN elemental and water contact angle analysis, and water vapour adsorption. The mesoporous silica-supported Rh catalyst with a Rh:octyl group ratio of 1:15 and a 1.6 nm pore diameter exhibited the highest catalytic activity in water: the yield of the 1,4-addition reaction increased to 93%, whereas a yield of only 31% was observed using the catalyst without the co-immobilized octyl groups. The mesoporous silica-supported Rh catalyst exhibited broad applicability to a range of arylboronic acids and enones.

Introduction

Recently, with the development of economic technology and improvement of living standards, green, sustainable development strategies in the field of synthetic chemistry attracted attention [1]. However, most organic syntheses are performed in organic solvents extracted from petroleum feedstocks. The use of organic solvents not only consumes petroleum feedstock, but also pollutes the environment. In contrast, water is cheap, non-toxic, abundant, and green. Although the low solubilities of organic compounds in water leads to low reactivities during organic reactions, the immiscibility of water and organic compounds also simplifies separation and purification [2,3]. Therefore, water is still attracting the attention of numerous scientific communities. One of the most efficient methods to achieve a green,

sustainable catalytic synthetic strategy involves replacing organic solvents in organic syntheses, such as acid- [4,5] or metal-catalysed [6,7] reactions, with water to reduce the harmful environmental effects of organic solvents. One of the most effective strategies in the design of water-tolerant catalysts is the introduction of hydrophobic or amphiphilic groups close to the catalytically active sites [4-7]. For example, Uozumi *et al.* reported a Rh-chiral diene complex immobilised on amphiphilic polystyrene-polyethylene glycol (PEG) resin which catalysed 1,4-addition reactions in water [7a].

Rh-catalysed 1,4-addition effectively provides β -substituted carbonyl compounds. Recently, numerous efforts to develop catalysts for 1,4-addition reactions were reported. Since 1997, Miyaura *et al.*, Hayashi *et al.*, Uozumi *et al.*, etc. developed various novel homo- and heterogeneous Rh catalysts that catalysed 1,4-addition reactions in organic and aqueous solvents [8,9]. Our group also reported a cooperative catalytic system, wherein the Rh complex and tertiary amine were co-immobilized on the surface of silica to catalyse 1,4-addition reactions [10]. This report demonstrates the combination of supported Rh complex and co-immobilized tertiary amine group for efficient catalysis in organic solvent. Our strategy for catalyst design, i.e. the accumulation of multiple functionalities on the same surface [11], should extend to the introduction of hydrophobic/amphiphilic units on the silica surface bearing active Rh complexes in water.

Herein, we developed mesoporous silica (MS)-supported Rh complexes alongside organic functional groups to catalyse 1,4-addition reactions in water (Eq. 1). The co-immobilized organic groups may significantly improve the catalysis of 1,4-addition

^a Department of Chemical Science and Engineering, School of Materials and Chemical Technology, Tokyo Institute of Technology, 4259 Nagatsuta-cho, Midori-ku, Yokohama 226-8502, Japan

^b Department of Chemistry and Life Science, Yokohama National University 79-5 Tokiwadai, Hodogaya-ku, Yokohama 240-8501, Japan
*E-mail: motokura-ken-xw@ynu.ac.jp

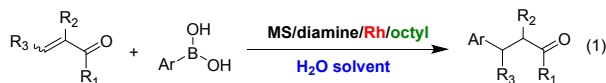
^c Institute for Catalysis, Hokkaido University, Kita 20, Nishi 10, Kita-ku, Sapporo 001-0021, Japan

^d Renewable Energy Research Center, National Institute of Advanced Industrial Science and Technology, 2-2-9 Machiikedai, Koriyama, Fukushima 963-0298, Japan

^e Graduate School of Arts and Sciences, International Christian University, Mitaka, Tokyo 181-8585, Japan

† Electronic Supplementary Information (ESI) available. See DOI: 10.1039/x0xx00000x

reactions in water and provide higher yields, overcoming the low solubilities of organic substrates in water. We characterised the catalyst using spectroscopic techniques and analysed the influences of the MS pore structure and other factors on the catalytic activity and range of substrates of the 1,4-addition reaction in water.

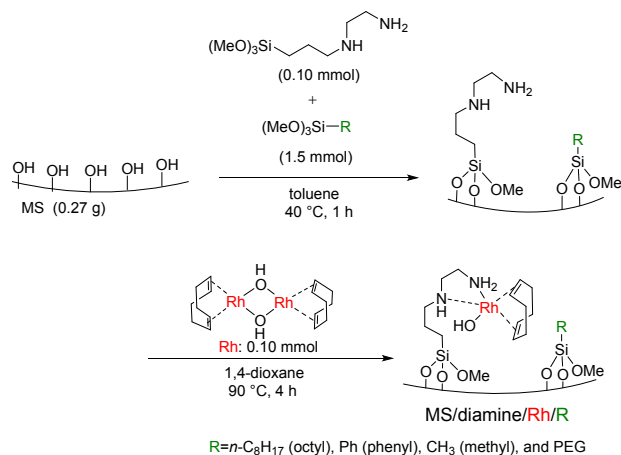


Results and Discussion

Catalyst preparation and characterization

The MS support was synthesised *via* a sol-gel process using a primary amine (*n*-octyl- (C8), *n*-decyl- (C10), *n*-dodecyl- (C12), or *n*-octadecylamine (C18)) as a structure-directing agent [12]. Depending on the length of the carbon chain of the structure-directing agent, the corresponding MS supports exhibit pore diameters of 16, 19, 23, and 31 Å, respectively. These MSs are denoted as MS(Cn), where Cn is the carbon chain length of the primary amine used. Other silica supports (SBA-15 with a pore size of 72 Å and nonporous silica (Aerosil 300)) were also used as catalyst supports and compared with the MS supports. The physical properties of the synthesised silica supports are summarised in **Table S1** (Supporting Information) [13].

The co-immobilization of the Rh complexes and organic groups on the surface of MS is shown in **Scheme 1**. The MS-supported diamines and organic groups (MS/diamine/R) are prepared *via* the simple silane coupling of [3-(2-aminoethylamino)propyl]trimethoxysilane and organic groups with the silane on the silica surface. A 1,4-dioxane solution containing [Rh(cod)OH]₂ (cod = cyclooctadiene) is then added to the MS/diamine/organic groups, yielding MS-supported Rh complexes alongside organic groups (MS/diamine/Rh/R). *n*-Octyl (*n*-C₈H₁₇), phenyl (Ph), methyl (–CH₃), and PEG organic functional groups were used.



Scheme 1. Preparation of MS/diamine/Rh/R (R = organic functionality).

Table 1. Elemental analyses of the MS-supported Rh catalysts with different organic groups.

Catalyst	Organic group (R : Rh)	Element (mmol / g) ^c		
		C	N	Rh
MS(C8)/diamine/Rh ^b	-	5.8	0.6	0.312
MS(C8)/diamine/Rh/octyl	Octyl (15:1)	27.5	0.3	0.156
MS(C8)/diamine/Rh/octyl	Octyl (10:1)	17.0	0.5	0.214
MS(C8)/diamine/Rh/octyl	Octyl (5:1)	16.1	0.6	0.277
MS(C8)/diamine/Rh/octyl	Octyl (1:1)	10.6	0.7	0.314
MS(C8)/diamine/Rh/methyl	Methyl (15:1)	8.1	0.6	0.324
MS(C8)/diamine/Rh/phenyl	Phenyl (15:1)	21.3	0.5	0.215

^a The amounts of C and N were measured using elemental analysis, and Rh was determined using inductively coupled plasma atomic emission spectroscopy (ICP-AES). ^b Data from [10c].

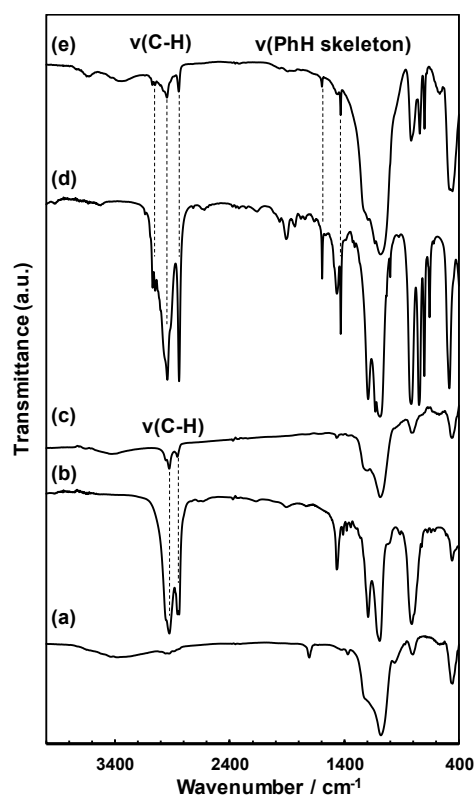


Fig. 1 FT-IR spectra of (a) MS(C8)/diamine/Rh, (b) trimethoxyoctylsilane, (c) MS(C8)/diamine/Rh/octyl, (d) trimethoxyphenylsilane, and (e) MS(C8)/diamine/Rh/phenyl.

The elemental analyses of the prepared MS(C8)-supported Rh catalysts with different organic groups and ratios of Rh and octyl groups are summarised in **Table 1**. The C content of MS/diamine/Rh/octyl increases with increasing organic functional group content. The N/Rh ratio of the MS/diamine/Rh/organic group is ~2, indicating the formation of a diamine Rh complex (**Table 1**). As the pore size of the silica support increases, no significant changes in the C and N

amounts are observed, suggesting that the pore size of the silica support does not affect the mounting of the Rh complexes and octyl groups (Table S2, Supporting Information). The Fourier transform infrared (FT-IR) spectra (Fig. 1) confirm the presence of organic groups on the surfaces of the MS/diamine/Rh/R catalysts. As shown in Figs. 1(b) and (c), the spectra of trimethoxyoctylsilane and MS(C8)/diamine/Rh/octyl exhibit similar peaks at $\sim 2900\text{ cm}^{-1}$, which are assigned to $\nu(\text{C-H})$. The spectra of trimethoxyphenylsilane (Fig. 1(d)) and MS(C8)/diamine/Rh/phenyl (Fig. 1(e)) also exhibit similar peaks at $\sim 2900\text{ cm}^{-1}$. In addition, two peaks representing the benzene skeleton vibration are also observed at 1590 and 1650 cm^{-1} before and after immobilisation of the phenyl group [14]. These results indicate the immobilisation of the octyl and phenyl groups while maintaining their structures.

The coordination environments of the Rh complexes of the MS-supported catalysts were analysed using Rh *K*-edge X-ray absorption fine structure (XAFS) spectroscopy. Fig. 2(A) shows the X-ray absorption near edge structure (XANES) spectra of the MS-supported Rh catalysts with different organic groups, MS(C8)/diamine/Rh/octyl (1:15) after the catalytic reaction, and the corresponding reference samples. The features of the XANES spectra of all MS-supported Rh catalysts [(a)–(e)] are similar to those of the spectrum of $[\text{Rh}(\text{cod})\text{OH}]_2$ (f), but differ from those of the spectra of Rh_2O_3 (g) and Rh foil (h), indicating the structures of the surface Rh complexes. Fig. 2(B) shows the Fourier-transformed extended X-ray absorption fine structure (FT-EXAFS) spectra of the MS-supported Rh catalysts and the corresponding reference samples. The FT-EXAFS spectra of the MS-supported Rh catalysts [(a)–(e)] exhibit strong signals at $\sim 1.6\text{ \AA}$. This signal is very close to those representing Rh–C/O observed in the spectra of $[\text{Rh}(\text{cod})\text{OH}]_2$ (f) and Rh_2O_3 (g), but different from those representing Rh–Rh and Rh–O–Rh bonds. These XANES and FT-EXAFS results indicate that the types of organic functional groups do not strongly affect the coordination structures of the Rh species on the surfaces. As shown in Figs. S1 and S2, Supporting Information, the pore size of the support and the Rh:octyl ratio do not affect the local structures of the Rh complexes. The curve fitting (CF) analysis results of the EXAFS spectra of the MS-supported Rh catalysts are summarised in Table 2. For the MS-supported Rh catalysts, whether they contain different organic groups, pore sizes, or ratios of Rh and octyl groups, the coordination numbers (*N*) and bond distances (*R*) are approximately 7 and $2.06\text{--}2.09\text{ \AA}$, respectively. These values are consistent with those previously reported for an MS-supported Rh complex [10c], indicating the formation of diamino Rh complexes on the MS surfaces. The effect of pore size on the CF results is scarcely observed, and the octyl:Rh ratio does not affect the local structures of the Rh complexes, as shown in Table S3, Supporting Information.

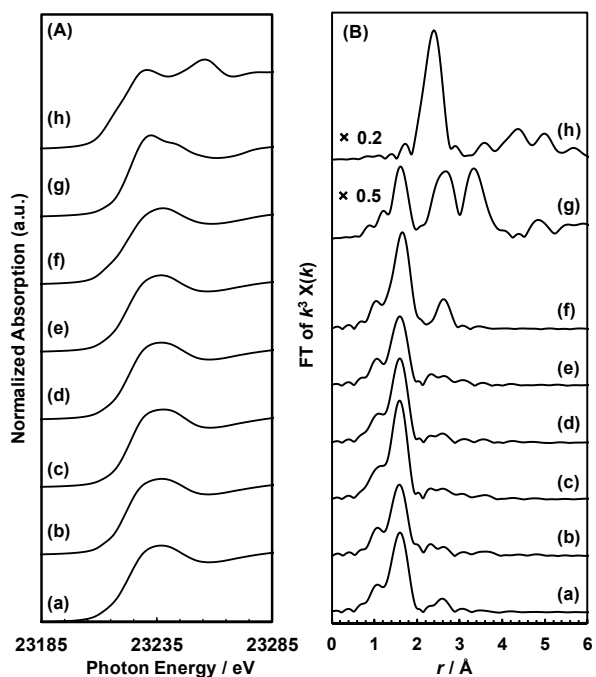


Fig. 2 (A) Rh *K*-edge XANES and (B) k^3 -weighted FT-EXAFS spectra of (a) MS(C8)/diamine/Rh/octyl, (b) used MS(C8)/diamine/Rh/octyl, (c) MS(C8)/diamine/Rh/methyl, (d) MS(C8)/diamine/Rh/phenyl, (e) MS(C8)/diamine/Rh, (f) $[\text{Rh}(\text{cod})\text{OH}]_2$, (g) Rh_2O_3 , and (h) Rh foil.

Table 2. Curve fitting analyses of the prepared MS-supported Rh catalysts.^a

Sample	<i>N</i> ^b	<i>R</i> (Å) ^c	$\Delta\sigma^2$ (Å ² × 10 ⁻³) ^d	ΔE_0 (eV) ^e	Rf (%) ^f
MS(C8)/diamine/Rh ^g	6.7 ±1.2	2.09 ±0.01	5.81 ±0.29	-4.1 ±2.3	0.80
MS(C8)/diamine/Rh/ Octyl	7.0 ±1.5	2.07 ±0.01	3.63 ±0.58	-3.0 ±2.8	0.92
MS(C8)/diamine/Rh/ methyl	6.9 ±1.3	2.06 ±0.01	2.03 ±0.48	-3.6 ±2.8	0.50
MS(C8)/diamine/Rh/ Phenyl	6.8 ±1.5	2.07 ±0.01	2.03 ±0.48	-3.0 ±2.8	0.79
MS(C10)/diamine/Rh/ octyl	6.7 ±1.4	2.07 ±0.01	3.63 ±0.58	-3.7 ±2.8	0.78
MS(C12)/diamine/Rh/ octyl	6.8 ±1.5	2.08 ±0.01	3.46 ±0.58	-2.6 ±2.8	0.93
MS(C18)/diamine/Rh/ octyl	6.9 ±1.5	2.07 ±0.01	3.80 ±0.58	-3.2 ±2.8	0.98
SBA-15/diamine/Rh/ Octyl	6.8 ±1.5	2.07 ±0.01	2.96 ±0.63	-2.7 ±2.8	0.85
MS(C8)/diamine/Rh/ octyl used ^h	6.6 ±1.3	2.07 ±0.01	4.80 ±0.40	-3.8 ±2.7	1.73
$[\text{Rh}(\text{cod})\text{OH}]_2$; ⁱ Rh-C	4	2.09			
Rh-O	2	2.07			

^a Fourier transform and Fourier-filtering regions were limited, with $\Delta k \approx 3.0\text{--}11 \text{ \AA}^{-1}$ and $\Delta r \approx 1.2\text{--}2.2 \text{ \AA}$, respectively. ^b Coordination number. ^c Bond distance between absorber and backscattering atoms. ^d Debye–Waller (DW) factor relative to that of the reference. ^e Inner potential correction to account for the difference in the inner potentials of the sample and reference. ^f Goodness of curve fit. ^g Data from [10c]. ^h Recovered catalyst after the 1,4-addition reaction. ⁱ Average values of crystallographic data are reported [15].

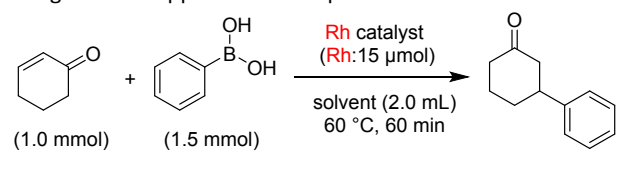
Catalysis of 1,4-addition reactions of arylboronic acids

1,4-Addition reactions of 1.0 mmol of cyclohexenone and 1.5 mmol of phenylboronic acid catalysed using the prepared MS(C8)-supported Rh catalysts were conducted, as shown in **Table 3**. The yield using MS(C8)/diamine/Rh (Entry 1) in water is only 31%, whereas that using MS(C8)/diamine/Rh/octyl is 93% (Entry 2). Time-course analysis of these reaction clearly indicates that this difference is due to a higher reaction rate of the catalyst with octyl group (Fig. S5). Other supported Rh complexes with organic functionalities, such as PEG, phenyl, and methyl (Entries 3–5), also exhibit superior activities in water compared to that of the catalyst without organic groups. In contrast, in dioxane/H₂O, the catalytic performances of MS(C8)/diamine/Rh and MS(C8)/diamine/Rh/octyl are almost identical, as shown in Entries 6 and 7. Therefore, the MS-supported Rh catalysts with organic groups effectively promote the 1,4-addition reaction in water, and MS(C8)/diamine/Rh/octyl exhibits the optimal activity (Entry 2, 93% yield). Using MS(C8)/diamine/Rh/PEG, the ether functionality mimics the surrounding environment of the Rh complex in the 1,4-dioxane solution, whereas a simple hydrophobic environment using the octyl group exhibits higher catalytic performance.

After confirming that the octyl group is a superior organic group for the 1,4-addition reaction in water, we examined the effect of the ratio of Rh to the organic group on the 1,4-addition reaction (**Fig. 3**). With an increase in the ratio of Rh to organic groups, the catalytic activity of MS-supported Rh also gradually increases, whereas the catalytic activity is similar for each Rh:octyl ratio in 1,4-dioxane/water. Among the catalysts used, MS(C8)/diamine/Rh/octyl with the highest ratio (1:15) exhibits the highest catalytic activity. This octyl group amount is almost an upper limit because of the surface Si–OH density [13]. The hydrophobicities of the MS-supported Rh catalysts with different Rh:octyl group ratios were determined using the water contact angle, as shown in **Table 4**. The contact angle of the MS-supported Rh catalyst without octyl groups is almost zero, and the water droplets are rapidly absorbed by the sample. With an increase in the amount of octyl groups, the contact angles of the other catalysts gradually increase, indicating that the hydrophobicity of the catalyst gradually increases. The water vapour adsorption isotherms of MS(C8), MS(C8)/diamine/Rh, and MS(C8)/diamine/Rh/octyl were also measured to determine the hydrophobicities of the mesopores (**Fig. 4**). For MS(C8) and MS(C8)/diamine/Rh, the water adsorption rate increases at approximately $P/P_0 = 0.3$, whereas no large water

uptake is observed at $P/P_0 \leq 0.85$ on MS(C8)/diamine/Rh/octyl. We also evaluated adsorption capacity of organic substrate into the MS internal surface. Under the aqueous reaction conditions, 2.2 mmol g⁻¹ of cyclohexanone was adsorbed into the MS/diamine/Rh/octyl, whereas adsorption amount was only 0.14 mmol g⁻¹ with MS/diamine/Rh. Therefore, the organic groups protect the active Rh centres from water and simultaneously absorb organic substrates into the mesopores, which leads to an increase in the substrate molecule concentration around Rh.

Table 3. Effect of solvent on the 1,4-addition reaction catalysed using the MS-supported Rh complexes.^a



Entry	Solvent	Catalyst	Conv. of cyclohexenone (%) ^b	Yield (%) ^b
1	H ₂ O	MS(C8)/diamine/Rh	66	31
2	H ₂ O	MS(C8)/diamine/Rh/octyl	> 99	93
3	H ₂ O	MS(C8)/diamine/Rh/PEG	>99	84
4	H ₂ O	MS(C8)/diamine/Rh/phenyl	65	51
5	H ₂ O	MS(C8)/diamine/Rh/methyl	74	61
6	dioxane/H ₂ O	MS(C8)/diamine/Rh	97	98
7	dioxane/H ₂ O	MS(C8)/diamine/Rh/octyl	97	97

^a Reaction conditions: cyclohexenone (1.0 mmol), phenylboronic acid (1.5 mmol), Rh catalyst (Rh: 1.5 μmol), solvent (2 mL: H₂O or 10:1 dioxane/H₂O), 60 °C, 60 min. The ratio of Rh to organic functional groups was 1:15, except for MS(C8)/diamine/Rh/PEG (Rh:PEG = 1:5) because of the large PEG precursor, (TMS)₃SiC₃H₆(OC₂H₄)_{9–12}OCH₃. ^b Determined by ¹H NMR spectroscopy using 1,3,5-triisopropylbenzene as the internal standard.

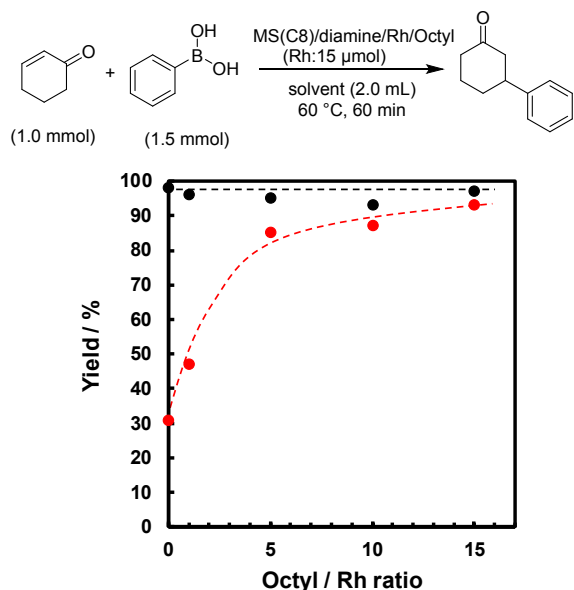


Fig. 3 Effect of the octyl/Rh ratio on the 1,4-addition reaction. Red: in water, black: in 10/1 dioxane/water.

Table 4. Water contact angles of the SiO₂/diamine/Rh/octyl catalysts.^a

Rh : octyl	Water contact angle (°)
1 : 0	n.d. ^b
1 : 1	77 ± 2
1 : 5	104 ± 1
1 : 10	112 ± 2
1 : 15	131 ± 1

^a Samples were prepared from powdered catalyst samples using a tablet press at 20 MPa. ^b Water droplets are rapidly absorbed by the catalyst.

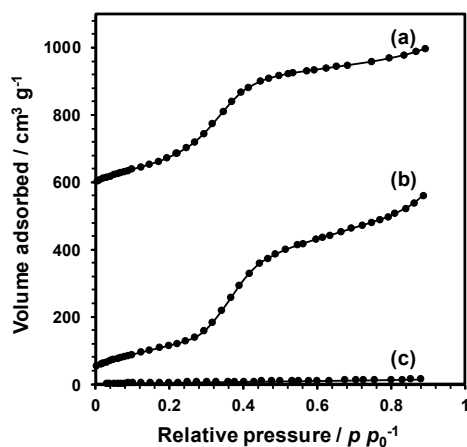


Fig. 4 H₂O adsorption isotherms of the MS(C8) samples measured at 25 °C. (a) Bare MS(C8), (b) MS(C8)/diamine/Rh, and (c) MS(C8)/diamine/Rh/octyl.

The effect of the pore size of the support on the 1,4-addition reactions catalysed using the MS-supported Rh complex catalysts was investigated, and the results are presented in **Fig. 5**. As the pore size of the MS support increases, the yield of the 1,4-addition reaction gradually decreases. MS(C8)/diamine/Rh/octyl exhibits the highest catalytic activity, whereas the nonporous silica-supported Rh catalyst exhibits a much lower performance even with the co-immobilized octyl group. This may be because the small-mesopore structure with octyl groups on the internal surface may effectively shield the attached Rh complexes from water. Immobilisation of hydrophobic groups on the catalyst surface is common in the field of aqueous catalysis; however, this is the first study to clarify the effect of pore size on catalysis in water assisted by hydrophobic groups.

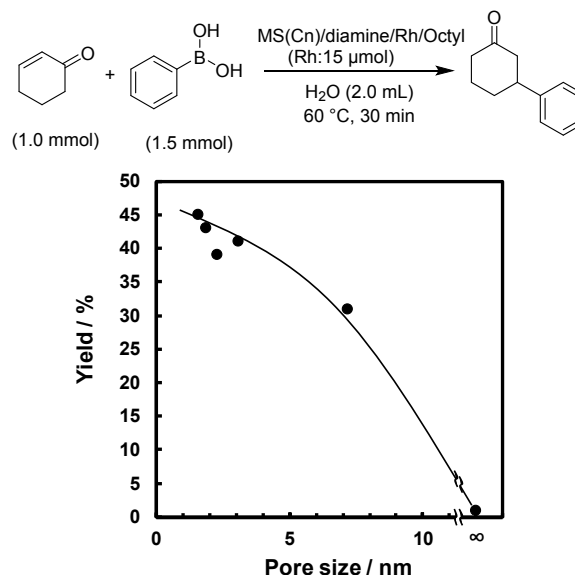
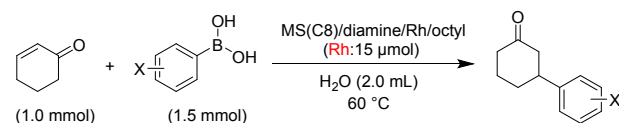


Fig. 5 Effect of the pore size of the support on the MS/diamine/Rh/octyl-catalysed 1,4-addition reaction. ∞: nonporous silica was used as the support.

Using MS(C8)/diamine/Rh/octyl (1:15), we investigated the substrate range of 1,4-addition of phenylboronic acids with cyclohexenone in water, and the results are summarised in **Table 5**. Phenylboronic acid with electron-donating or -withdrawing groups reacts smoothly in water with high yields of 96–99% (Entries 2–9). In addition to the *para* position, *ortho/meta*-substituted phenylboronic acid reacts effectively with cyclohexenone (Entries 4 and 5). Phenylboronic acid with a NO₂ substituent also yields the corresponding cyclohexanone in a high yield (87%) (Entry 10). Therefore, the substituent on

phenylboronic acid, whether it is an electron-withdrawing or -donating group or another organic group, exhibits no adverse effect on the 1,4-addition reaction in water, and the yield of the corresponding product is very good. The initial reaction rate of substituted phenylboronic acid was then investigated. Phenylboronic acid with an electron-withdrawing group exhibits a higher reaction rate than that of phenylboronic acid with an electron-donating group; the ρ value is >1 , based on the Hammett plot (Fig. S3). This trend is similar to that of the homogeneous Rh complex-catalysed reaction [8], suggesting a similar reaction mechanism of Rh–OH with the cod ligand. For the recovered catalyst, the XAFS analysis, XANES and FT-EXAFS spectra (Fig. 2), and curve-fitting analysis results (Table 2) are almost the same as those of the fresh catalyst. Hence, the cod ligand may coordinate to the Rh site during the reaction. The recovered catalyst may be reusable; however, it exhibits a slightly lower reaction rate ($1.3 \times 10^{-2} \text{ mmol min}^{-1}$) compared with that of the fresh catalyst ($1.5 \times 10^{-2} \text{ mmol min}^{-1}$). No leaching of Rh into the water was observed using inductively coupled plasma atomic emission spectroscopy (ICP-AES); the amount of Rh in the solution was lower than the detection limit. No significant change of local Rh structure after catalysis was observed in XAFS analysis (Figure 2). These results indicate that the main reason for the deactivation might be adsorption of organic compounds around the active Rh center and/or internal surface of mesopore due to the hydrophobic environment.

Table 5. Scope of arylboronic acid in the 1,4-addition reaction in water.^a



Entry	Arylboronic acid	Time (h)	Conv. of cyclohexenone (%) ^b	Yield (%) ^b
1	Ph-	1	> 99	93
2	4-F-C ₆ H ₄ -	1	95	96
3	4-Cl-C ₆ H ₄ -	1	>99	96
4	2-Cl-C ₆ H ₄ -	1	>99	>99
5	3-Cl-C ₆ H ₄ -	1	>99	>99
6	4-CF ₃ -C ₆ H ₄ -	1	>99	>99
7	4-CH ₃ O-C ₆ H ₄ -	1	> 99	99
8	4-CH ₃ -C ₆ H ₄ -	3	> 99	97
9	4-CH ₃ C(O)-C ₆ H ₄ -	3	> 99	96
10 ^c	4-NO ₂ -C ₆ H ₄ -	6	> 99	87
11	B(OH) ₂ 	1	>99	99
12	B(OH) ₂ 	6	67	60

^aReaction conditions: cyclohexenone (1.0 mmol), arylboronic acid (1.5 mmol), MS(C8)/diamine/Rh/octyl (Rh: 1.5 μmol), H₂O (2 mL), 60 °C. ^bDetermined by ¹H NMR using internal standard technique and 1,3,5-triisopropylbenzene was used as internal standard. ^cH₂O (4 mL).

Table 6. Scope of unsaturated carbonyl compounds on the 1,4-addition reaction of phenylboronic acid in water^a

Entry	Enone	Time (h)	Conv. of cyclohexenone (%) ^b	Yield (%) ^b
1		1	> 99	93
2		3	61	60
3		3	>99	80
4		3	>99	>99
5		3	>99	87
6 ^c		3	>99	>99
7 ^d		6	67	67

^aReaction conditions: enone (1.0 mmol), phenylboronic acid (1.5 mmol), MS(C8)/diamine/Rh/octyl (Rh: 1.5 μmol), H₂O (2 mL), 60 °C. ^bDetermined by ¹H NMR using internal standard technique and 1,3,5-triisopropylbenzene was used as internal standard. ^c100 °C. ^d90 °C.

The substrate range of the unsaturated carbonyl compounds in the 1,4-addition reaction is shown in Table 6. Various unsaturated ketones, such as 3-octen-2-one and chalcone, exhibit good-to-high yields under the catalysis of MS(C8)/diamine/Rh/octyl (Entries 1–4). These hydrophobic substrates showed much lower reactivity with the supported catalyst without octyl group. The reactions with unsaturated nitriles also occur smoothly, resulting in high yields of the corresponding products (Entries 5 and 6). Unsaturated aldehydes may also produce higher yields, although longer reaction times are required (Entry 7). The catalyst system exhibits broad applicability and strong catalytic activity in the 1,4-addition reactions of various arylboronic acids and unsaturated carbonyl substrates in water.

Conclusions

In conclusion, MS-supported Rh catalysts with organic groups efficiently catalysed 1,4-addition reactions of phenylboronic acids and unsaturated ketones in water. MS(C8)/diamine/Rh/octyl (1:15) with a smaller MS support pore size and more octyl groups increases the yield of the 1,4-addition reaction in water from 31% to 93%, with the catalytic activity significantly improved. The 1,4-addition reaction catalysed by MS/diamine/Rh/octyl exhibits a broad substrate scope in terms of phenylboronic acids and unsaturated ketones. MS/diamine/Rh/octyl is highly effective in catalysing the 1,4-addition reaction in water, with good potential for applications.

Conflicts of interest

There are no conflicts to declare.

Acknowledgements

This study was supported by a Japan Society for the Promotion of Science Grant-in-Aid for Scientific Research on Innovative (grant no. JP20H04804) and Transformative Research Areas (grant no. JP21H05099), the Yazaki Memorial Foundation for Science and Technology, Cooperative Research Program of the Institute for Catalysis, Hokkaido University (Grant No. 21B1018), the Noguchi Institute, and the Tokuyama Science Foundation. This work was also supported by a PRESTO grant (No. JPMJPR17SA) awarded by the Japan Science and Technology Agency. XAFS was conducted with the approval of the Photon Factory Advisory Committee (Proposal No. 2020G033).

Notes and references

- P. Anastas and N. Eghbali, *Chem. Soc. Rev.*, 2010, **39**, 301–312.
- A. Filly, A.S. Fabiano-Tixier, C. Louis, X. Fernandez and F. Chemat, *C. R. Chimie*, 2016, **19**, 707–717.
- T. Okuhara, *Chem. Rev.*, 2002, **102**, 3641–3666.
- (a) F. Liu, K. Huang, A. Zheng, F.-S. Xiao and S. Dai, *ACS Catal.*, 2018, **8**, 372–391. (b) S. Navalon, A. Dhakshinamoorthy, M. Alvaro and H. Garcia, *Chem. Rev.*, 2014, **114**, 6179–6212. (c) K. Nakajima and M. Hara, *ACS Catal.*, 2012, **2**, 1296–1304. (d) J. Shi, L. Zhang and Z. Cheng, *Catal. Surveys Asia*, 2021, **25**, 279–300.
- Examples for acid-catalyzed reactions in water, see: (a) S.M.A.H. Siddiki, T. Toyao, K. Kon, A. S. Touchy and K. Shimizu, *J. Catal.*, 2016, **344**, 741–748. (b) N. Nuryono, A. Qomariyaha, W. Kimb, R. Otomoc, B. Rusdiarsoa and Y. Kamiyac, *Mol. Catal.*, 2019, **475**, 110248. (c) P. Kasinathan, C. Lang, E. M. Gaigneaux, A. M. Jonas, and A. E. Fernandes, *Langmuir*, 2020, **36**, 13743–13751. (d) L. Li, H. Yue, S. Zhang, Y. Huang, W. Zhang, P. Wu, Y. Ji and F. Huo, *ACS Appl. Mater. Interfaces*, 2019, **11**, 9919–9924. (e) Y. Zhong, P. Zhang, X. Zhu, H. Li, Q. Deng, J. Wang, Z. Zeng, J.-J. Zou and S. Deng, *ACS Sustainable Chem. Eng.*, 2019, **7**, 14973–14981. (f) M. Hara, T. Yoshida, A. Takagaki, T. Takata, J. N. Kondo, S. Hayashi and K. Domen, *Angew. Chem. Int. Ed.*, 2004, **43**, 2955–2958. (g) K. Inumaru, T. Ishihara, Y. Kamiya, T. Okuhara and S. Yamanaka, *Angew. Chem. Int. Ed.*, 2007, **46**, 7625–7628. (h) J. Ji, G. Zhang, H. Chen, S. Wang, G. Zhang, F. Zhang and X. Fan, *Chem. Sci.*, 2011, **2**, 484–487. (i) J. Wei, L. Zou and J. Li, *New J. Chem.*, 2016, **40**, 4775–4780. (j) P. Kasinathan, C. Lang, S. Radhakrishnan, J. Schnee, C. D'Haese, E. Breynaert, J. A. Martens, E. M. Gaigneaux, A. M. Jonas and A. E. Fernandes, *Chem. Eur. J.*, 2019, **25**, 6753–6762. (k) T. Okada, K. Miyamoto, T. Sakai and S. Mishima, *ACS Catal.*, 2014, **4**, 73–78. (l) H. Miura, S. Kameyama, D. Komori and T. Shishido, *J. Am. Chem. Soc.*, 2019, **141**, 1636–1645.
- (a) T. Kitanosono, K. Masuda, P. Xu and S. Kobayashi, *Chem. Rev.*, 2018, **118**, 679–746. (b) R. Akiyama and S. Kobayashi, *Chem. Rev.*, 2009, **109**, 594–642. (c) S. Minakata and M. Komatsu, *Chem. Rev.*, 2009, **109**, 711–724. (d) M.-O. Simon, C.-J. Li, *Chem. Soc. Rev.*, 2012, **41**, 1415–1427.
- Examples for metal-catalyzed reactions in water, see: (a) G. Shen, T. Osako, M. Nagaosa and Y. Uozumi, *J. Org. Chem.*, 2018, **83**, 7380–7387. (b) M. Vafaezadeh, J. Schaumlöffel, A. Lösch, A. D. Cuyper and W. R. Thiel, *ACS Appl. Mater. Interfaces*, 2021, **13**, 33091–33101. (c) F. Zhang, X. Wu, C. Liang, X. Li, Z. Wang and H. Li, *Green Chem.*, 2014, **16**, 3768–3777. (d) H. Shintaku, K. Nakajima, M. Kitano and M. Hara, *Chem. Commun.* 2014, **50**, 13473–13476. (e) P. Barbaro and F. Liguori, *Chem. Rev.*, 2009, **109**, 515–529. (f) Y. Uozumi and K. Shibatomi, *J. Am. Chem. Soc.*, 2001, **123**, 2919–2920. (g) T. Yasukawa, H. Miyamura and S. Kobayashi, *J. Am. Chem. Soc.*, 2012, **134**, 16963–16966. (h) Y. Uozumi, H. Danjo and T. Hayashi, *J. Org. Chem.*, 1999, **64**, 3384–3388. (i) M. Chen, C. Liang, F. Zhang and H. Li, *ACS Sustainable Chem. Eng.*, 2014, **2**, 486–492.
- Homogeneous Rh catalysts for 1,4-addition reactions: (a) M. Sakai, H. Hayashi and N. Miyauro, *Organometallics*, 1997, **16**, 4229–4231. (b) Y. Takaya, M. Ogasawara, T. Hayashi, M. Sakai and N. Miyauro, *J. Am. Chem. Soc.*, 1998, **120**, 5579–5580. (c) S. Sakuma and N. Miyauro, *J. Org. Chem.*, 2001, **66**, 8944–8946. (d) M. Kuriyama and K. Tomioka, *Tetrahedron Lett.*, 2001, **42**, 921–923. (e) M. T. Reetz, D. Moulin and A. Gosberg, *Org. Lett.*, 2001, **3**, 4083–4085. (f) T. Hayashi, M. Takahashi, Y. Takaya and M. Ogasawara, *J. Am. Chem. Soc.*, 2002, **124**, 5052–5058. (g) J.-G. Boiteau, A. J. Minnaard and B. L. Feringa, *J. Org. Chem.*, 2003, **68**, 9481–9484. (h) A. Kina, K. Ueyama, and T. Hayashi, *Org. Lett.*, 2005, **7**, 5889–5892. (i) T. Korenaga, K. Osaki, R. Maenishi and T. Sakai, *Org. Lett.*, 2009, **11**, 2325–2328. (j) X. Hu, M. Zhuang, Z. Cao and H. Du, *Org. Lett.*, 2009, **11**, 4744–4747. (k) A. Kina, Y. Yasuhara, T. Nishimura, H. Iwamura and T. Hayashi, *Chem. Asian J.*, 2006, **1**, 707–711. (l) A. Kina, H. Iwamura and T. Hayashi, *J. Am. Chem. Soc.*, 2006, **128**, 3904–3905.
- Heterogeneous Rh catalysts for 1,4-addition reactions: (a) Y. Uozumi and M. Nakazono, *Adv. Synth. Catal.*, 2002, **344**, 274–277. (b) Y. Otomaru, T. Senda and T. Hayashi, *Org. Lett.*, 2004, **6**, 3357–3359. (c) F. Neatu, M. Besnea, V. G. Komvokis, J.-P. Genêt, V. Michelet, K. S. Triantafyllidis and V. I. Pârvulescu, *Catal. Today*, 2008, **139**, 161–167. (d) P. Handa, T. Witula, P. Reis and K. Holmberg, *ARKIVOC*, 2008, 107–118. (e) M. L. Kantam, V. B. Subrahmanyam, K. B. S. Kumar, G. T. Venkanna and B. Sreedhar, *Helv. Chim. Acta.*, 2008, **91**, 1947–1953. (f) P. Handa, K. Holmberg, M. Sauthier, Y. Castanet and A. Mortreux, *Microporous Mesoporous Mater.*, 2008, **116**, 424–431. (g) R. Jana and J. A. Tunge, *Org. Lett.*, 2009, **11**, 971–974. (h) R. Jana and J. A. Tunge, *J. Org. Chem.*, 2011, **76**, 8376–8385. (i) K. Motokura, N. Hashimoto, T. Hara, T. Mitsudome, T. Mizugaki, K. Jitsukawa and K. Kaneda, *Green Chem.*, 2011, **13**, 2416–2422. (j) T. Yasukawa, H. Miyamura and S. Kobayashi, *J. Am. Chem. Soc.*, 2012, **134**, 16963–16966. (k) T. Hara, N. Fujita, N. Ichikuni, K. Wilson, A. F. Lee and S. Shimazu, *ACS Catal.*, 2014, **4**, 4040–4046. (l) T. Yasukawa, A. Suzuki, H. Miyamura, K. Nishino and S. Kobayashi, *J. Am. Chem. Soc.*, 2015, **137**, 6616–6623. (m) T. Yasukawa, H. Miyamura and S. Kobayashi, *ACS Catal.*, 2016, **6**, 7979–7988. (n) T. Yasukawa, Y. Saito, H. Miyamura, S and Kobayashi, *Angew. Chem. Int. Ed.*, 2016, **55**,

- 8058-8061. (o) H. Miyamura, K. Nishino, T. Yasukawa and S. Kobayashi, *Chem. Sci.*, 2017, **8**, 8362-8372. (p) G. Shen, T. Osako, M. Nagaosa and Y. Uozumi, *J. Org. Chem.*, 2018, **83**, 7380-7387.
- 10 (a) H. Noda, K. Motokura, W. -J. Chun, A. Miyaji, S. Yamaguchi and T. Baba, *Catal. Sci. Technol.*, 2015, **5**, 2714-2727. (b) H. Noda, K. Motokura, Y. Wakabayashi, K. Sasaki, H. Tajiri, A. Miyaji, S. Yamaguchi and T. Baba, *Chem. Eur. J.*, 2016, **22**, 5113-5117. (c) K. Motokura, K. Hashiguchi, K. Maeda, M. Nambo, Y. Manaka and W.-J. Chun. *Mol. Catal.*, 2019, **472**, 1-9.
- 11 K. Motokura, S. Ding, K. Usui and Y. Kong, *ACS Catal.*, 2021, **11**, 11985-12018.
- 12 P. T. Tanev and T. J. Pinnavaia, *Science.*, 1995, **267**, 865-867.
- 13 (a) K. Motokura, M. Ikeda, M. Nambo, W.-J. Chun, K. Nakajima and S. Tanaka, *ChemCatChem.*, 2017, **9**, 2924-2929. (b) K. Motokura, M. Ikeda, M. Kim, K. Nakajima, S. Kawashima, M. Nambo, W.-J. Chun and S. Tanaka, *ChemCatChem.*, 2018, **10**, 4536-4544.
- 14 J. Gu, C. Liang, J. Dang, X.-D. Meng, L. Tang, Y. Li and Q.-Y. Zhang, *RSC Adv.*, 2016, **6**, 57357-57362.
- 15 R. E. Marsh, M. Kapon, S. Hu and F. H. Herbstein, *Acta Crystallogr., Sect. B: Struct. Sci.*, 2002, **58**, 62-77.